Pushing the Data Rate of Practical VLC via Combinatorial Light Emission

Yanbing Yang   Jun Luo   Chen Chen   Zequn Chen   Wen-De Zhong   Liangyin Chen

Abstract—*Visible Light Communication* (VLC) systems relying on commercial-off-the-shelf (COTS) devices have gathered momentum recently, due to the pervasive adoption of LED lighting and mobile devices. However, the achievable throughput by such practical systems is still several orders below those claimed by controlled experiments with specialized devices.In this paper, we engineer CoLight aiming to boost the data rate of the VLC system purely built upon COTS devices. CoLight adopts COTS LEDs as its transmitter, but it innovates in its simple yet delicate driver circuit wiring an array of LED chips in a combinatorial manner. Consequently, modulated signals can directly drive the on-off procedures of individual chip groups, so that the spatially synthesized light emissions exhibit a varying luminance following exactly the modulation symbols. To obtain a readily usable receiver, CoLight interfaces a COTS PD with a smartphone through the audio jack, and it also has an alternative MCU-driven circuit to emulate a future integration into the phone. The evaluations on CoLight are both promising and informative: they demonstrate a throughput up to 80 kbps at a distance of 2 m, while suggesting various potentials to further enhance the performance.

Index Terms—Visible Light Communication, Combinatorial Emission, Spatial Modulation, Intensity Modulation

◆

1 INTRODUCTION

VISIBLE light communication has long been envisioned as an alternative to RF communications, and it keeps attracting attentions given the increasing scarcity of RF spectrum resources. In the past decade, experimental VLC setups with highly sophisticated constructions have been able to deliver a throughput up to a few Gbps [2], yet none of them have been put into practice by far. At the meantime, practical VLC systems relying on commercial-off-the-shelf (COTS) devices have been gaining their momentum, mainly thanks to the pervasive adoption of *Light Emitting Diodes* (LEDs) lighting [3] and mobile devices (e.g., smartphones). Whereas these practical developments admit immediate deployments, the achieved throughput, only at kbps level (e.g., [4], [5], [6], [7], [8], [9]) due to the low sampling rate resulted from using cameras as the receivers and the low-order modulation schemes adopted on the transmitter side, is far below that claimed by the experimental setups. Fortunately, we believe that there is a big room for improving the practical systems to close the gap between them and the experimental setups.

To our understanding, one major reason that prevents those high-performance experimental setups from becoming practical is the nonlinear nature of LEDs [10], [11], [12]. Essentially, the relation between LED input (voltage or current) and output (intensity or luminance) can be highly nonlinear, and this distortion is affected by LED types

and ambient conditions (e.g., temperature) as well. Existing solutions overcome this nonlinearity by either sacrificing spectral efficiency or applying complicated processing logic or circuits [13], [14]. While the former method (already adopted by practical VLC systems) yields simple but inefficient modulations (e.g, OOK [15] or PPM [16]) that largely confine the throughput, the latter significantly increases the system complexity and hence reduces the robustness to, for example, ambient noises and interferences, making its feasibility very questionable in practice.

Another obstacle to deploy high-performance VLC setups is their high costs. These experimental setups always utilize high-power LEDs and high-sensitivity *Photo-Diodes* (PDs), and they may also apply special lenses and filters [2], [17]; all these imply a high cost. In reality, VLC has certain obvious drawbacks: it is directional and requires *Line-of-Sight* (LoS) links thus cannot provide a sufficient coverage as WiFi does, and it is invasive as light emissions with a high intensity can be very disturbing to human users. As a result, a reasonable choice of VLC transmitters would be the existing lighting infrastructure, rather than any specifically designed modules similar to the WiFi access points. In the context of piggybacking on a lighting infrastructure, the cost incurred by high-performance VLC setups appears prohibitively high, and some of the incurred complications (e.g., lenses and filters) become inapplicable.

Unfortunately, recently proposed practical VLC systems are all too conservative in addressing aforementioned challenges [18], [15], [19], [20], [6], resulting in a throughput only up to a few kbps. They mostly resort to low-order modulations that trade spectral efficiency for avoiding nonlinearity, and they exploit the rolling-shutter effect of CMOS cameras (readily usable for all smartphones but badly performing in frequency response) to suppress the system complexity. DarkLight [16] adopts PPM for modulation and a PD as the receiver, but the spectral efficiency of PPM is too low to

●Yanbing Yang, Zequn Chen and Liangyin Chen are with College of Computer Science/Institute for Industrial Internet Research, Sichuan University, P.R. China. Email: {yangyanbing, chenliangyin}@scu.edu.cn.
●Jun Luo is with School of Computer Science and Engineering, Nanyang Technological University, Singapore. Email: junluo@ntu.edu.sg.
●Chen Chen is with School of Microelectronics and Communication Engineering, Chongqing University, P.R. China. Email: c.chen@cqu.edu.cn.
●Wen-De Zhong is School of Electrical and Electronic Engineering, Nanyang Technological University, Singapore. Email: ewdzhong@ntu.edu.sg.
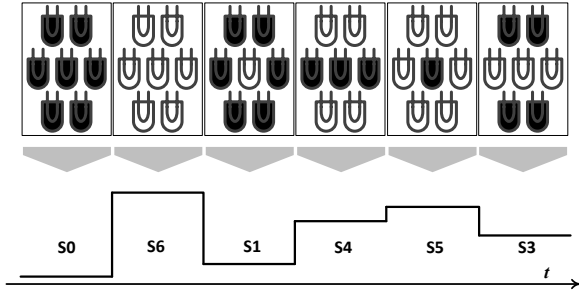
Fig. 1. The idea of combinatorial light emissions: the emissions from multiple LEDs are controlled so that the spatially synthesized intensities represent respective modulation symbols.

Fig. 2. LED Nonlinearity.

achieve a high throughput within an affordable bandwidth, and it is not clear how to interface PD with a COTS device. ReflexCode [6] slightly increases the modulation order at the cost of involving multiple LED luminaires, which may confine the system applicability. Apparently, more aggressive designs are key to close the gap between practical deployments and experimental setups.

To this end, we design CoLight to probe the limit of COTS VLC systems from both transmitter and receiver sides. To enable higher-order modulations given the LED nonlinearity, we revisit the idea of spatial synthesizing for intensity modulation, but we innovate in a compact circuit design that generates up to 256-PAM (*Pulse Amplitude Modulation*) with a COTS LED array. Essentially, the transmitter of CoLight wires an array of LED chips in a combinatorial manner and directly drives the on-off procedures of individual chip groups according to the modulation symbols. As a result, the signal patterns get linearly "translated" to varying luminance, thanks to the spatially synthesized light emissions, as shown in Fig. 1. In order to relax the bottleneck at CMOS cameras while still maintain practicality (i.e., the ability of using smartphones as receivers), we propose two approaches to interface a PD with a smartphone: a plug-in solution using the audio jack and a potential (future) integration into the phone. In summary, we make the following major contributions:

- A novel transmitter built upon COTS LEDs to generate high-order modulations (up to 256-PAM) without being troubled by LED nonlinearity.
- A calibration scheme to automatically handle the LED chip diversity in transmitter production.
- A practical receiver interfacing a PD with a smartphone through the audio jack, and achieving a high-speed transmission via specially designed coding and decoding schemes.
- An MCU-driven receiver emulating a more advanced design that can be potentially integrated into smartphones for a much higher performance.
- Extensive evaluations with CoLight prototype to not only demonstrate its promising performance but also provide guidelines for future developments.

CoLight is not meant to chase the best performance, but rather aims to explore different aspects of realizing the spatial synthesizing technology in practice. It provides us with a better understanding of potentials and limits of the COTS VLC systems in general. In the following, we first introduce the background in Section 2. The transmitter and
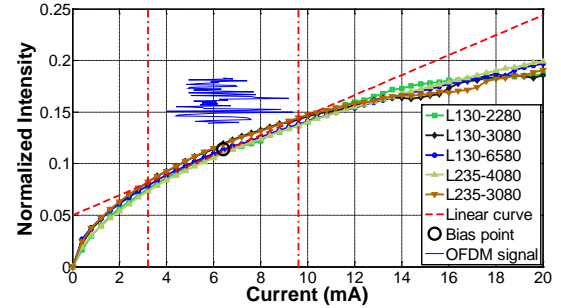
receivers of CoLight are then presented in Section 3 and 4, respectively. We further report and discuss the extensive evaluations in Section 5. We finally give a brief literature review in Section 6 and conclude our paper in Section 7.

2 PRELIMINARY AND MOTIVATION

We set up the background for developing CoLight in this section. We first briefly explain the LED nonlinearity and the potential solution based on spatial light synthesizing. Then we study the performance of COTS LED in term of frequency response, for both single LED chip and chip groups. We finally discuss the challenge of interfacing a PD with smartphones.

2.1 Nonlinearity of LED

It is well known that an LED has strong nonlinearity [10], [11], [12], making it very hard to realize high-order modulations. Most proposals confine the (luminance) dynamic range of LEDs to a very narrow section so as to retain linearity [2], [21] (the OFDM signal shown in Fig. 2), but they require a very high transmitting power or special lens/filters to achieve an adequate *Signal-to-Noise Ratio* (SNR) at the receiver. This method is obviously not feasible for COTS VLC piggybacking on an existing light infrastructure subject to certain luminance control. Other proposals resort to predistortion or postdistortion [13], [14] to rectify the nonlinearity, they yet require complicated processing circuits, and even worse, these circuits have to be fine-tuned to suit individual LEDs given their different manifestations of nonlinearity. Fig. 2 shows a few typical LED input response curves that are measured based on several types of LEDs chips; the nonlinearity and its varying manifestations with different LED types are quite evident.

Alternatively, varying luminance (thus realizing intensity modulations) can be made effective by spatially synthesizing the light emissions from a group of LEDs with a varying size [22]. Under this method, individual LEDs only experience an On-Off process like OOK so that nonlinearity does not matter at all. However, existing implementations all stay at small scales and mostly apply high power LEDs, with only channel quality measurements that are of little practical significance [22], [23]. In Section 3, we will present our transmitter prototype based on the same principle but enabling full-fledged data transmissions, but before that, we need to understand the performance of COTS LEDs under high frequencies, especially when they are grouped.
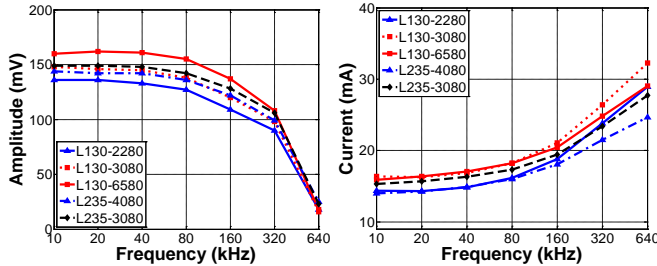
(a) Recv. light intensity. (b) Driving current.

Fig. 3. Frequency response of single LEDs. (a) Received light intensity decreases with frequency, while (b) driving current increases at the same time.
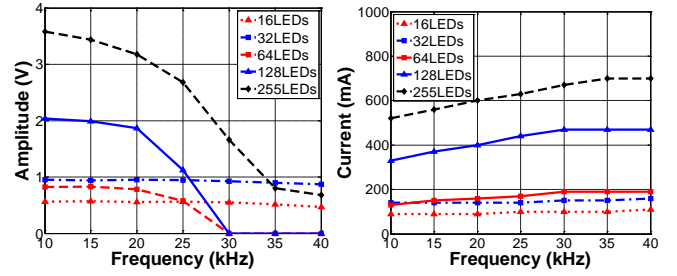
2.2 Frequency Response of Single LEDs

In order to control the On-Off process of LED chips, existing LED luminaires have to be upgraded so that control signals can be exerted on individual chips. In this section, we test the frequency response of the COTS illumination LEDs controlled by low-cost transistors[1]. We use a function generator to generate OOK signals with the frequency varying from 10 kHz to 640 kHz to drive the LEDs, and we report the received light intensity by PDA10A [24] without any filters in Fig. 3(a). We also investigate the performance by various types of LEDs with different color temperatures, ranging from 2200 K (warm white) to 6500 K (cool white). We observe that color temperature does not have a major impact, and the cut-off frequency at around 320 kHz is evident. This limit is set by the phosphor coating used for COTS illuminating LEDs [25]: though LED chips usually have a relatively fast switching speed, they are slowed down by that of the phosphor coating. Moreover, we employ a multimeter to measure the average DC current consumed by the LEDs and plot the outcome in Fig. 3(b). It is intuitive to observe that a higher frequency increases the power consumption due to the LED's parasitics. Both results suggest that chasing a higher throughput by increasing frequency may not be efficient for COTS illumination LEDs, motivating us to target at higher-order modulations.

2.3 Grouping Degrades Performance

Implementing spatially light synthesizing by controlling individual LED chips may cause an over-complicated driver circuit, but grouping the chips wisely can significantly reduce the driver complexity. For example, controlling 7 chips to obtain 8 levels of luminance only requires 3 control signals (rather than 7) if the chips are put into 3 groups with sizes 4, 2, 1, respectively. However, the performance bottleneck now becomes the largest group, because all chips in it are controlled by a transistor and an isolator is needed to protect the MCU from the high voltage control signal.

Here we test the frequency response of LED groups under typical cascade and parallel connections used by CoLight transmitter detailed in Section 3. The same transistor is used for the control purpose and a low-cost isolator TLP293-4 [26] is put between the MCU and driver. Fig. 4 reports the experiment results given the same metrics used for Fig. 3.

1. We use the extremely low-cost (0.06 USD per chip) and small-size transistor MMSS8050-H-TP in order to suppress the potential cost for upgrading LED luminaires.

(a) Recv. light intensity. (b) Driving current.

Fig. 4. Frequency response degradation caused by grouped LEDs.

The drastic reduction in working frequency (compared with single LEDs measured in Section 2.2) mostly attributes to the low-cost isolator. Also, the saturation of the transistor limits the driving current and hence the input power. Consequently, the overall low-cost design of CoLight allows for a safe working frequency up to 25 kHz. Obviously, replacing the transistor and isolator with their high-performance (thus high-cost) counterparts would increase this frequency, but this is out of the scope of our CoLight objective, which aims to exploit higher-order modulations for improving spectral efficiency.

2.4 Audio Jack as VLC Receiver

An ideal COTS VLC receiver should be integrated into smartphones (like the WiFi module). While we will develop a specific circuit to emulate such a potential integration, we also like to have a receiver immediately applicable to smartphones, which naturally leads to the adoption of audio jack. Using audio jack as a VLC receiver is not new, but existing proposals only support a very low throughput, e.g., 0.7 kbps reported in [27]. Fig. 5 shows a typical VLC receiver based on audio jack. The internal bias voltage drives the reception circuit with a photodiode and parallel resistor, allowing the ADC directly acquires the analog signals generated by the receiver and making it seemingly straightforward to act as a plug-and-play receiver [27], [28], [29].

However, the coupling capacitor, i.e., C1 in Fig. 5, limits the DC component of input signal hence strongly affecting the performance of amplitude-based high-order modulation schemes such as PAM. Fig. 6 graphically compares the signal sampled from the audio interface with that sampled by a digital oscilloscope at similar sample rates: 44.1 kHz for the former and 50 kHz for the latter. Apparently, the signal distortion caused by audio sampling can seriously affect on the demodulation performance. Therefore, CoLight requires a new coding/decoding scheme to mitigate this distortion.
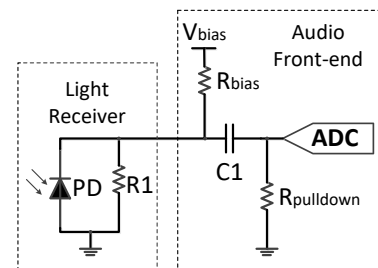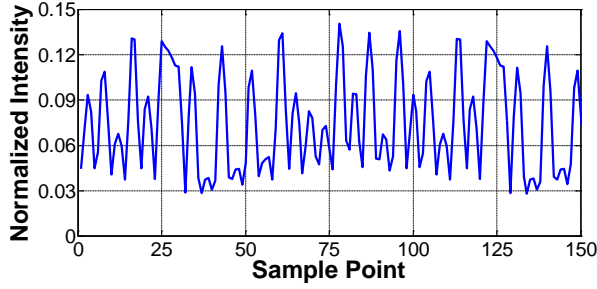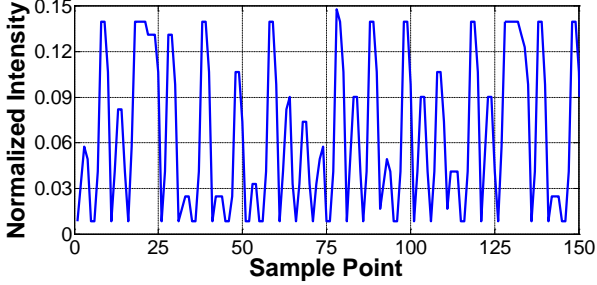

Fig. 5. Circuit diagram of a VLC receiver via smartphone audio jack, including a model of the audio front-end and a photodiode receiver.

(a) Data sampled by phone's audio interface.

(b) Data sampled by a digital oscilloscope.

Fig. 6. Sampled signals by the smartphone's audio interface comparing with those sampled by a digital oscilloscope.

3 SYNLIGHT TRANSMITTER

In this section, we detail the theoretical analysis, design and implementation of CoLight transmitter.

3.1 Front-end with Reduced Control

As mentioned in Sec. 2.1, exerting control on individual LED chips can unnecessarily increase the driver complexity. Therefore, we wire the chips in a combinatorial manner, i.e., we group them so that the output optical power grows in a stepping manner of a power of two, as shown in Fig. 7(a). As a result, an LED array with N chips only requires $\log N$ control signals. Moreover, such an arrangement leads to a natural "translation" from digital bits to modulation intensities. For example, the first group (containing only one chip) is driven by the least significant bit of one byte (assuming 255 chips in the array to be driven by a *codebook* containing one byte control codes), and the most significant bit drives the last group with 128 chips. The physical layout of the LED chips in our CoLight prototype is illustrated in Fig. 7(b), where we choose an octagon shape to emulate a common
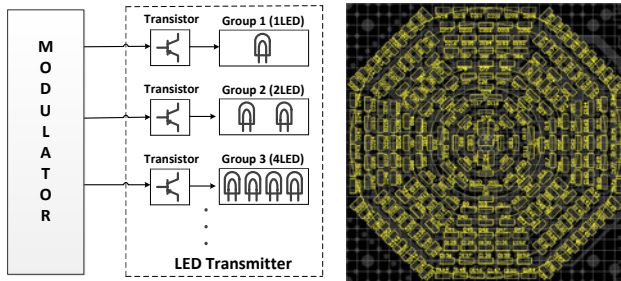
(a) The combinatorial grouping of LED chips.

(b) Layout of 255 LED chips.

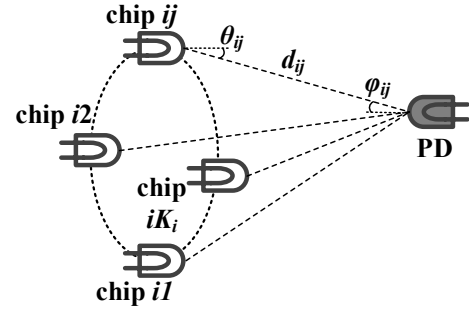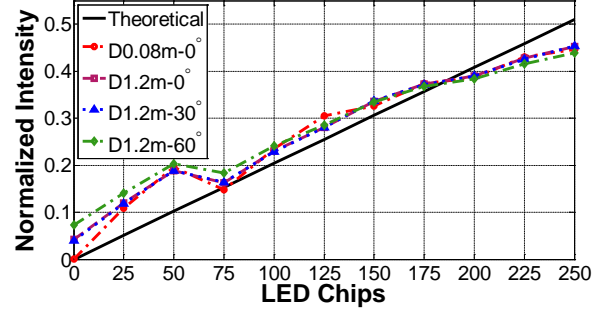Fig. 7. The front-end of CoLight transmitter.

Fig. 8. Modeling the combinational light emissions from the i-th group containing K_i LED chips.

Fig. 9. Normalized RLIs: theoretical analysis and experiment measurements. We measure the RLIs at two distances (0.08 m and 1.2 m) and also three view angles at the longer distance. The differences between the analysis and measurements are mainly due to component diversity and circuit configurations.

LED luminaire[2] with a disk face, and we symmetrically place the first group at the center and the last group at the periphery.

3.2 Combinational Light Emissions

We study the performance of spatial light synthesizing through both modeling and experiments. Fig. 8 illustrates the principle of spatial synthesizing of K_i LED chips in a group. Following the common practice [30], we assume that the emission of each chip follows a Lambertian radiation pattern. Considering only the LoS component and without using the optical filter and lens, the optical channel DC gain between the j-th chip of the i-th group and the PD is calculated as

$$h_{ij} = \frac{(m+1)A}{2\pi d_{ij}^2} \cos^m(\theta_{ij})\cos(\varphi_{ij}), \qquad (1)$$

where m is the Lambertian emission order given by $m = -\ln 2/\ln(\cos(\Theta))$ with Θ being the semi-angle at half power of each chip, A is the active area of the PD, d_{ij} is the transmission distance between the chip and the PD, θ_{ij} and φ_{ij} are the emission angle and the incident angle, respectively. If the incident light is outside the field-of-view of the receiver, the corresponding channel gain becomes zero.

In the proposed combinational light emissions, all the LED chips have only two states, i.e., On and Off, so we have a binary control process $x_{ij}(t) \in \{0, 1\}$ for each chip. Assuming that a total of G groups of LEDs are used, the

2. This is partially inspired by the lighting infrastructure used in our institute, where each 16 m² office is lit by four LED luminaires each with 288 chips.

overall spatially synthesized light intensity at the PD can be obtained by

$$y(t) = \sum_{i=1}^{G} \sum_{j=1}^{K_i} R h_{ij} x_{ij}(t) + n(t), \qquad (2)$$

where R is the responsivity of the PD and $n(t)$ is the corresponding additive thermal and shot noises. The additive nature of Equation (2) confirms that the combinational effect of multiple On-Off control processes should lead to a linear increase in *Received Light Intensities* (RLIs), which is key to CoLight and is shown as the theoretical curve in Fig. 9. However, due to the component diversity and particular circuit configurations, the actually measured RLIs are not exactly linear, as shown in Fig. 9. Essentially, as individual LED chips may not be uniform in their output optical intensities, the overall RLIs start to deviate from the ideal linearity when various groups of chips are involved.

3.3 Adaptively Calibrated Emissions

Due to the chip diversity in production, the combinational light intensity is not strictly linear with the number of alight LED chips as shown in Fig. 9. Conventionally, we may fine-tune the driver circuit to rectify this,[3] but such a method is no difference from the predistortion applied to counter the inherent LED nonlinearity (see Section 2.1), i.e., every produced transmitter has to be manually calibrated, which is too cumbersome to meet the need for constructing large scale VLC systems in practice. A practical calibration should solely rely on adjustments on the software side.

Taking the advantage of CoLight's stepping power control ability, we propose an adaptive calibration to rectify the nonlinearity by only adjusting the modulation codebook. Given the original codebook C^{PAM}, the element c_i^{PAM}, where the subscript i refers to the i-th modulation symbol, is set to $\lfloor 255 \times i/M \rceil$ initially, with M denoting the modulation order. We let the transmitter step up the number of On chips from 0 to N (where N denotes the total number of chips), and we record the corresponding RLIs shown in Fig. 10(a) as "original". The recorded light intensities are stored in a
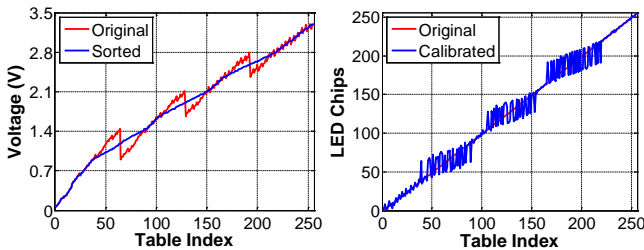
(a) RLIs before/after sorting.　(b) 256-PAM codebook before/after calibration.

Fig. 10. Adaptive calibration based on RLIs.

vector $\boldsymbol{\ell} = [\ell_0, \ell_1, \cdots, \ell_N]$, and the corresponding control code c_i is set in the codebook as $c_i = i$ assuming the system is linear. Now we sort $\boldsymbol{\ell}$ ascendingly and adjust the corresponding codes in the codebook $\boldsymbol{C}$: i.e., if ℓ_i and ℓ_j exchanged their positions after sorting, the value of c_i and c_j should also be exchanged. Finally, we go through the original codebook $\boldsymbol{C}^{\mathrm{PAM}}$ ascendingly and look up in the

---

3. Existing proposal [22] applies a current-limiting resistor to every chip group so as to enable the fine-tuning.

Algorithm 1: Adaptively calibration.

Data: M, N, $\boldsymbol{C}^{\mathrm{PAM}}$, $\tilde{\boldsymbol{\ell}}$, ϵ
Result: $\boldsymbol{C}^{\mathrm{PAM}}$
begin
  $\boldsymbol{C} \leftarrow \emptyset$; $\boldsymbol{\ell} \leftarrow \boldsymbol{0}$; $i \leftarrow 0$;
  while $i \leq N$ **do**
    Switch i LED chips on,
    measure and record ℓ_i as the RLI
    $c_i \leftarrow i$; $\boldsymbol{C} \leftarrow \boldsymbol{C} \cup \{c_i\}$; $i \leftarrow i + 1$;
  Sort $\boldsymbol{\ell}$ ascendingly and adjust $\boldsymbol{C}$ accordingly
  $i \leftarrow 0$; $k \leftarrow 0$
  while $i \leq M$ **do**
    while $|\tilde{\ell}_i - \ell_k| > \epsilon$ **do**
      $k \leftarrow k + 1$;
    $c_i^{\mathrm{PAM}} \leftarrow c_k$; $i \leftarrow i + 1$;

---

sorted $\boldsymbol{\ell}$ for the one ℓ_k that best represents c_i^{PAM} (using the expected light intensity $\tilde{\ell}_i$ as a reference and $\epsilon > 0$ as the error threshold), and we update the code c_i^{PAM} using the value of c_k. We summarize this adaptive calibration as pseudocodes in **Algorithm 1** and illustrate the outcome in Fig. 10(b). In Fig. 11, we use the calibrated 8-PAM as an example. According to Fig. 11(a), the RLIs are perfectly linear with respect to the PAM symbols after our calibration. The differences shown in Fig. 11(b) between expected codes and the adjusted codes clearly demonstrate the effect of calibration. For example, the symbol S3 (binary value 011) is expected to be produced by alighting 110 chips (corresponding to code 01101110), but the transmitter actually alights 90 chips (code 01011010) to retain the linearity after calibration. Note that this calibration procedure, with an assistance of a high-quality PD (we use PDA36A [31]), is fully automated without the need for human intervention, so it is totally suitable for massive production.
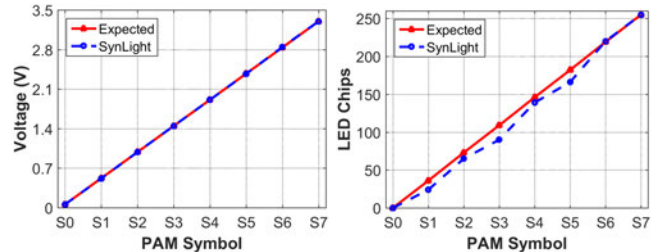
(a) 8-PAM symbols vs. their respective RLIs.　(b) 8-PAM symbols vs. their respective codes.

Fig. 11. Generated 8-PAM symbols using the calibrated codebook.

3.4 From Message to Modulated Light

In a typical unidirectional VLC system, messages are firstly coded by *Forward Error Correction* (FEC) codes into encoded packets to combat the packet loss. Subsequently, the encoded packets are modulated into control codes to drive the LED front-end, so as to embed digital information onto light intensity. We briefly illustrate the procedure of embedding messages into modulated light in Fig. 12(a) and the modulation circuit in Fig. 13(a). Moreover, VLC is considered as a secondary functionality piggybacking on a modern LED lighting infrastructure (as discussed in Section 1), so the
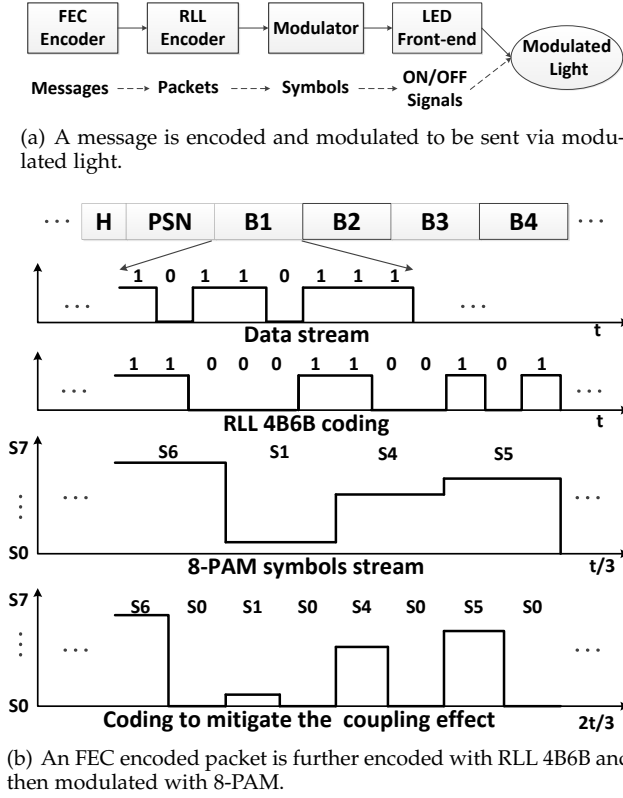
(a) A message is encoded and modulated to be sent via modulated light.

(b) An FEC encoded packet is further encoded with RLL 4B6B and then modulated with 8-PAM.

Fig. 12. Diagrams of coding and modulation for CoLight transmitter.
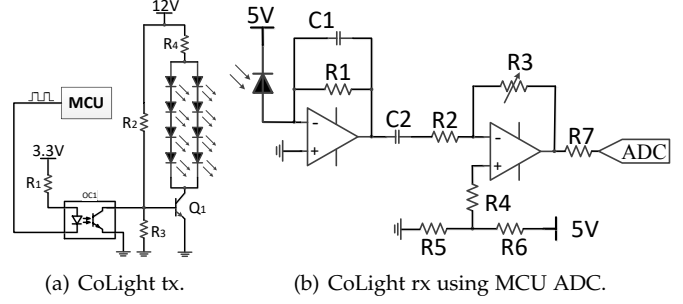

(a) CoLight tx.   (b) CoLight rx using MCU ADC.

Fig. 13. Circuit diagrams of CoLight transmitter and the receiver driven by an MCU. (a) Only a group of 8 LED chips is shown for brevity, and an optocoupler is used as the isolator. (b) The signal sensed by the PD is amplified by a transimpedance amplifier and a clamping amplifier, before sampled by the MCU ADC.

to maintain a stable amplitude from time to time. To mitigate the AC coupling effect caused by the capacitor, we propose a new coding based on 4B6B before modulation. The lowest part in Fig. 12(b) shows the designed coding: each significant symbol is followed by a S0 to convert any DC "plateau" to an AC falling edge, and adding S0 causes the sharpest edge possible under unipolar VLC. With this novel coding scheme, a CoLight receiver can avoid measuring the absolute amplitude value easily distorted by the AC coupling; it may instead detect the amplitude difference between any two adjacent symbols. Detailed decoding procedure is presented in Section 4.

4 SYNLIGHT RECEIVER

As the receiver from a practical VLC system, we would like it to be readily applicable to smartphones (the most pervasively used COTS mobile devices). However, high-speed communication modules need to be integrated into a phone, which is certainly beyond our reach. Therefore, we emulate such a potential integration via an MCU-driven circuit with two types of PDs as its front-ends, as shown in Fig. 13(b). We also interface a low-end PD to the phone's audio jack, confirming the readily usable nature of CoLight.

4.1 Packet Extraction via Header

As mentioned in Section 3.4, modulated light emissions carry encoded messages. The receiver uses a PD to sense these emissions and converts them to voltage signals sampled either by an MCU or by the audio interface of a smartphone. As VLC is asynchronous and one-way, each data packet contains a header to indicate the start of valid data transmissions. The receiver then recognizes data transmissions by detecting the headers. As shown in Fig. 14(a), a valid header has a relatively high light intensity and holds on for the longest time; we refer to Section 5.1 for more details on packet format. Before decoding, CoLight uses the first few samples (typically 200) to search for the maximum value of sampled data. Then it sets a rough threshold based on this maximum; this threshold, along with a typical duration, are used to detect headers. Here we empirically configure the 0.6 of the maximum value as the threshold to maximize the chances of detecting headers.

proposed VLC transmitter should avoid causing any visible flicker during data transmissions.

CoLight applies 4B6B *Run Length Limit* (RLL) line coding for its simplicity and DC balance [32]. 4B6B coding generates 6 encoded bits for each 4 data bits while maintaining no more than three successive "1" or "0", meaning that a half data byte (4 bits) require two 8-PAM symbols or one 64-PAM symbol. Under 8-PAM, a byte coded with 4B6B thus requires 4 symbols as shown in Fig. 12(b) (we refer to Table 4 in [32] for the 4B6B mapping). More detailed studies show that combining 4B6B with 8-PAM requires only 6 symbols (S1 to S6) out of 8-PAM; a phenomenon occurs similarly to 2^k-PAM with an odd k. Therefore, we can reduce 8-PAM scheme to 6- or 7-PAM[4] scheme that represents the same amount of information with less symbols. This reduced modulation scheme benefits SNR because of less light intensity steps within the same output range. In other words, we may increase the symbol distance to improve the signal strength and thus the data rate.

3.5 Coding for AC Coupling

As mentioned in Section 2.4, using the audio jack of a smartphone as a VLC receiver demands a special coding scheme to combat the signal distortion caused by the special construction of the audio front-end. Specifically, AC coupling could interfere modulated signals due to the coupling capacitor filtering the DC component, but amplitude-based modulation suffers the most as it requires the circuit output

---

4. Though 6-PAM is already sufficient, CoLight has to adopt a different coding scheme for the audio receiver explained in Section 3.5. So we use 7-PAM for audio jack receivers and 6-PAM for MCU-driven receivers.

4.2 Demodulation with Differential

Given the perfect linearity of a calibrated transmitter (see Section 3.3), using a threshold-based demodulation to handle the data sampled by MCU is rather straightforward, so we omit its discussion for brevity. In the following, we focus on the demodulation of the transmissions dedicated to the audio jack receiver. Once two adjacent headers are recognized, the demodulator starts examining the samples between the two headers with a window determined by the transmission frequency and sample rate. The demodulation procedure is triggered by the first minimum value point in the packet right after the header (SP marked by a black diamond in Fig. 14(b)). Meanwhile, CoLight detects all extreme points (i.e., local maximum and minimum points, EP marked by red $*$ in Fig. 14(b)) via the first order differences of the samples, as the first order differences cross zero around all extreme point. Two neighboring extreme points are then paired to derive the absolute difference in values (blue triangle) as shown in Fig. 14(c). According to the coding scheme described in Section 3.5, a local maximum represents a PAM symbol and a subsequent local minimum
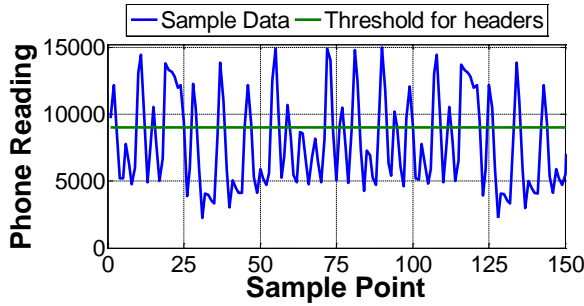
(a) The threshold for header detection.
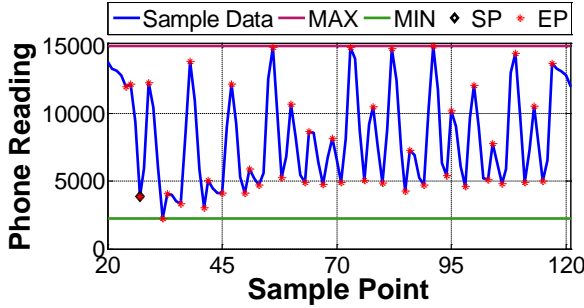
(b) Detect the starting point (SP), all local extreme points (EPs), and the global maximum and minimum points the packet.
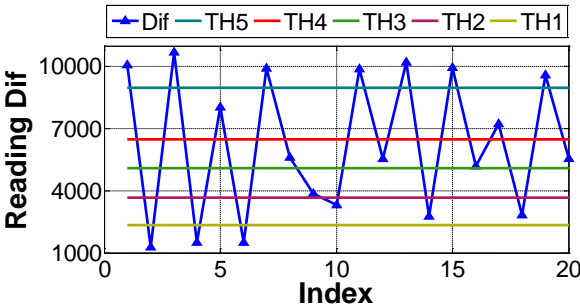
(c) Thresholds for symbol detection exploiting the differences between pairs of local maximum and minimum.

Fig. 14. CoLight demodulation procedure.

is the artificial zero created by our coding scheme to remove the DC component, so the difference between them indicates the symbol value. Moreover, we use the absolute difference between the global maximum and minimum in the packet, shown in Fig. 14(b) by two baselines, to proportionally configure thresholds for symbol detection. Once all symbols in the packet are recognized, the resulting candidate packet is then given to the FEC decoding for recovering the original message.

5 EVALUATIONS AND DISCUSSIONS

We extensively evaluate the performance of CoLight in this section, mainly in its real-life communication capacity. Based on the experiment results, we also seriously discuss the potentials and limits of CoLight, aiming to answer the question raised at the beginning.

5.1 Experiment Settings

Transmitter: We build CoLight's transmitter that integrates COTS components onto a 4-layer PCB as shown in Fig. 15. As already explained in Section 3.1, the transmitter front-end consists of 255 LED chips divided into 8 groups, and the i-th group has 2^i LED chips with $i = 0, 1, \cdots, 7$. The COTS illumination LED chip LUXEON 3014 ($\$0.26$ per chip) with a viewing angle of $116°$ is adopted to form this transmitter front-end. We employ a low-cost MSP430F2618 MCU as the controller to generate control signal for modulation. Two very low-cost 4-ch TLP293 optocouplers ($\$1.18$ each) are used to isolate the high voltage control signals from the MCU. Each LED group is directly controlled by one or more low-cost MMSS8050 transistors ($\$0.06$ each). As the maximum driving current of MMSS8050 is 1.5A, a single transistor may support only up to 16 LED chips in a group. So we need to use multiple transistors in parallel for groups with more than 16 chips to maintain a current below 1.5A for each transistor.

Receivers: Two types of CoLight's receiver are shown in Fig. 16; their respective circuit diagrams have already been illustrated in Fig. 5 and Fig. 13(b). Both receivers share the same SD3421 PD due to its wide FoV of $90°$ suitable for practical applications. For the receiver immediately applicable to smartphones shown in Fig. 16(a), we use an audio plug to directly connect it to the phone's audio jack so as to exploit the ADC and processors of the phone. We call this receiver Audio-RX; it has a default sample rate at 44.1 kHz. For the MCU-driven receiver shown in Fig. 16(b), we use the same MCU as the transmitter and build a transimpedance
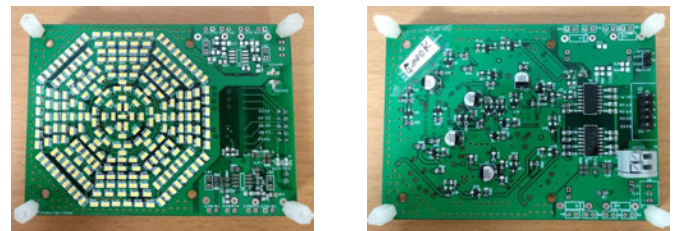
(a) Top layer.

(b) Bottom layer.

Fig. 15. Prototype of CoLight transmitter.

(a) Audio.   (b) MCU-driven.

Fig. 16. Prototypes of CoLight receiver. (a) Smartphone receiver via audio jack. (b) MCU-driven receiver with low-cost components, emulating a potential integration into phones.
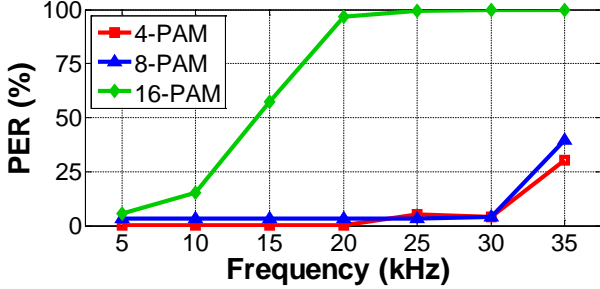

Fig. 17. PER with a varying transmission frequency under various PAM modulations by MCU-PDA36A-RX.

amplifier based on a low-cost AD8034 amplifier [33] to improve signal strength before ADC whose maximum sample rate is 200 kHz. In order to verify the impact of different front-ends, we also take PDA36A (already equipped with an amplification circuit) as another front-end. These two receivers are termed MCU-AD8034-RX and MCU-PDA36A-RX, respectively.

System configuration: We define each packet as containing a 4 bytes payload and identified by an 8-bit *Packet Sequence Number* (PSN), and all these are led by a header of 1 lowest symbol (S0) and 3 successive highest symbols (e.g., S7 for 8-PAM), as shown in Fig. 12(b) (the top). Since VLC is asynchronous and one-way, we employ a FEC scheme of Raptor coding to encode the message [34], and the coding overhead is set as 25%. Moreover, we adopt RLL 4B6B to avoid flicker of the LED front-end, as discussed in Section 3.4. To further handle the AC coupling of the audio interface, the new coding scheme proposed in Section 3.5 is applied on the transmitter side for the audio jack receiver. The transmission power is set to obtain an intensity of 400 lux at 1.2 m. At the receiver side, we use a Nexus 6 smartphone as the host to Audio-RX, and we leverage the phone's processor to handle packet decoding. For the MCU-driven receivers, we use them for sampling signal only but perform decoding offline on a PC, as the limited capability of the MCU results in a long latency in handling Raptor decoding. Each of our following experiments consists of 10 sessions and 320 packets (before FEC) are transmitted within each session. We report the average values over all sessions, except for data rates whose maximum values are also reported.

5.2 Transmission with Various PAM

We first evaluate the transmission ability of the CoLight under various modulation schemes, e.g., 4-, 8- and 16-

PAM, in this section. The MCU-PDA36A-RX is used as the receiver to achieve better perceived performance. The experiment results are shown in Fig. 17. Intuitively, CoLight can support 16-PAM at a transmission frequency of 10 kHz for safe communication with a *Packet Error Rate* (PER) lower than 25%. The reason why 16-PAM gets drastic degradation caused by increasing frequency is that higher frequency forces faster changes of LED status on the transmitter leading to stronger switching noise which may heavily distort the optical output of modulated symbols. Furthermore, the symbol distance of 16-PAM is largely reduced comparing with that of 4- or 8-PAM symbols, which is prone to be interfered by nonlinear output caused by chip diversity as mentioned in Section 3.2. In addition, low sampling rate and resolution of the MCU ADC also confine the reception ability of CoLight to recognize 16-PAM symbols. However, it is possible to improve the performance of high-order PAM by using more consistent LED chips and components in building the transmitter, should it be eventually integrated into smartphones with a professional design. As current CoLight prototype achieves a good tradeoff between transmission frequency and modulation order by 4- and 8-PAMs, i.e., with low PERs of around 5% at a maximum frequency of 30 kHz, we choose 4- and 8-PAMs for the remaining evaluations.

5.3 Demodulation under Ambient Light

In this section, we evaluate the demodulation performance of high order PAM under varying ambient light, since there may exist other non-VLC luminaires or sunlight through window in realistic VLC application scenarios. We change the illuminance from 400 lux (CoLight's transmitter alone as mentioned in Section 5.1) to 750 lux (with CoLight's transmitter and an extra luminaire), and we use a smartphone light meter APP monitoring the light intensity. As the Audio-RX has an AC-coupling capacitor which by default filters out DC component caused by ambient light, we here only report the results by two MCU-driven receivers for this evaluation shown in Fig. 18. Intuitively, our self-built receiver of MCU-AD8034-RX can automatically eliminate the interference by ambient light thanks to the AC coupling capacitor C2 shown in Fig. 13(b), which it is very similar with the coupling capacitor configured in smartphone's audio jack, yet we can customize its value to only remove the noise "DC" component but maintain the valid PAM symbols. As for the MCU-PDA36A-RX with DC coupling by default, we build a software high-pass filter into the
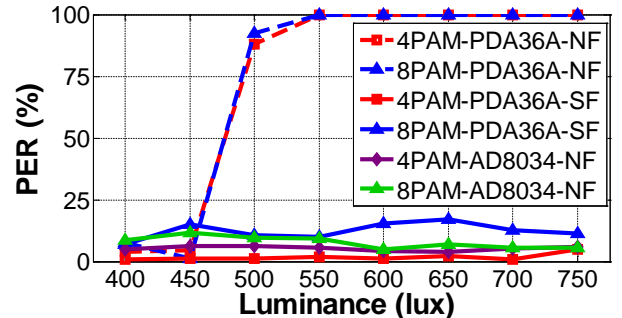

Fig. 18. Demodulation performance under ambient light by CoLight's MCU-driven receivers.
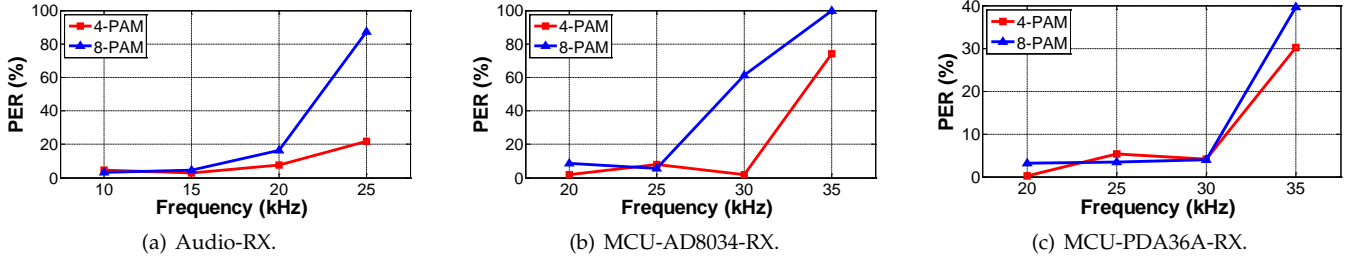
(a) Audio-RX. (b) MCU-AD8034-RX. (c) MCU-PDA36A-RX.

Fig. 19. PER with a varying transmission frequency.

(a) Audio-RX. (b) MCU-AD8034-RX. (c) MCU-PDA36A-RX.

Fig. 20. PER with a varying distance.

(a) Audio-RX. (b) MCU-AD8034-RX. (c) MCU-PDA36A-RX.
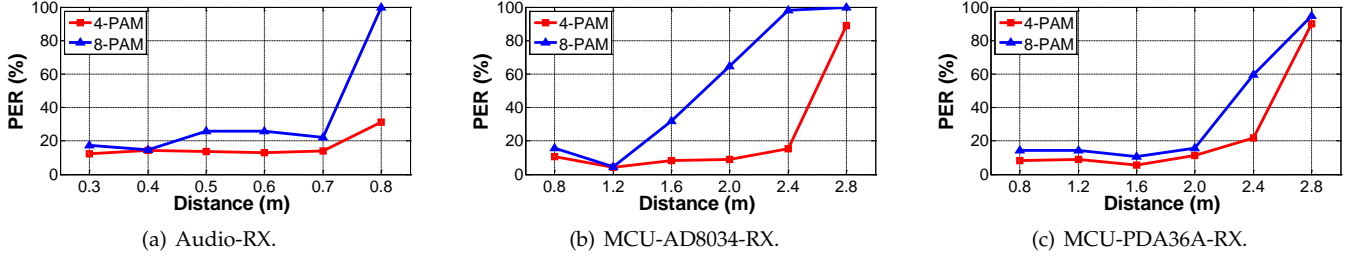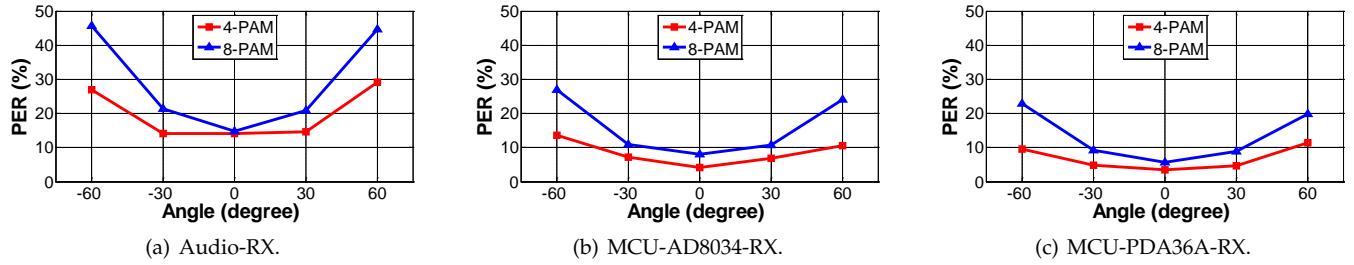
Fig. 21. PER with a varying viewing angle.

demodulator (labelled by PDA36A-SF in the figure), while we also consider the one without high-pass filter as a baseline with label of PDA36A-NF. Obviously, using the AC coupling capacitor or software high-pass filter makes CoLight substantially immune to ambient light.

5.4 Channel Property under PAM

In this section, we study the performance of CoLight given different channel settings and parameters.

5.4.1 Transmission Frequency

The operating frequency of the transmitter is the most important parameter that affects the data rate, so we first study its impact on the VLC channel quality, and we report the PER for three different receivers under various transmission frequency in Fig. 19. Here we position the Audio-RX at a distance of 0.4 m from the transmitter and the distance for MCU-driven receivers is 1.2 m. We vary the frequency from 10 kHz to 25 kHz for the Audio-RX and from 20 kHz to 35 kHz for another two receivers. The relatively low transmission frequency is confined by both the transmitter's feasible frequency studied in Section 2.3 and the receivers' sample rate. Although CoLight's transmitter is able to generate up to 256-PAM, the decreasing symbol distance makes it very hard to demodulate the signals beyond 8-PAM at a reasonable distance.

As expected, Audio-RX can only support a frequency up to 20 kHz given its sample rate at 44.1 kHz. One may expect that the 200 kHz sample rate of both MCU-AD8034-RX and MCU-PDA36A-RX would improve the performance a lot, but there are two catches. On one hand, the quality of PD certainly matters, as at least 5 kHz more can become usable by using a better PD. On the other hand, as PAM signal occupies a very wide bandwidth (due to its square waveform), 200 kHz may not be considered as oversampling under a 30 kHz transmission frequency, especially for high-order PAMs: our observation through a digital oscilloscope suggests that 25 kHz 16-PAM would require a sample rate of almost 1 MHz. In the following, we fix a transmission frequency of 20 kHz for Audio-RX and 25 kHz for MCU-AD8034-RX and MCU-PDA36A-RX.

5.4.2 Distance and View Angle

We also evaluate PERs of 4-PAM and 8-PAM with respect to both communication distance and (receiver) view angle; the results are reported in Fig. 20 and Fig. 21, respectively. We vary the distance from 0.3 m to 0.8 m for Audio-RX and from 0.8 m to 2.8 m for the MCU-driven receivers. It is quite clear that using an amplifier can greatly increase the communication distance, confirmed by comparing Fig. 20(a) with 20(b), and a better PD may further help as shown by Fig. 20(c). Apparently, a high-quality receiver front-end (PD) and a sufficient signal amplification/conditioning are crucial for increasing communication distance in a real-life deployment of a COTS VLC system.

Setting the distances as 0.4 m for Audio-RX and 1.2 m for the MCU-driven receivers, we further examine the PER by changing the viewing angle within $[-60, 60]^\circ$ for all

TABLE 1
PER Performance under mobile scenarios

	Audio-RX			MCU-AD8034-RX			MCU-PDA36A-RX		
	VM	PM	HM	VM	PM	HM	VM	PM	HM
4-PAM (%)	21.2	20.6	28.8	22.5	25.6	34.0	18.2	19.9	20.2
8-PAM (%)	35.5	33.9	43.4	34.4	27.7	43.9	20.7	22.5	25.7

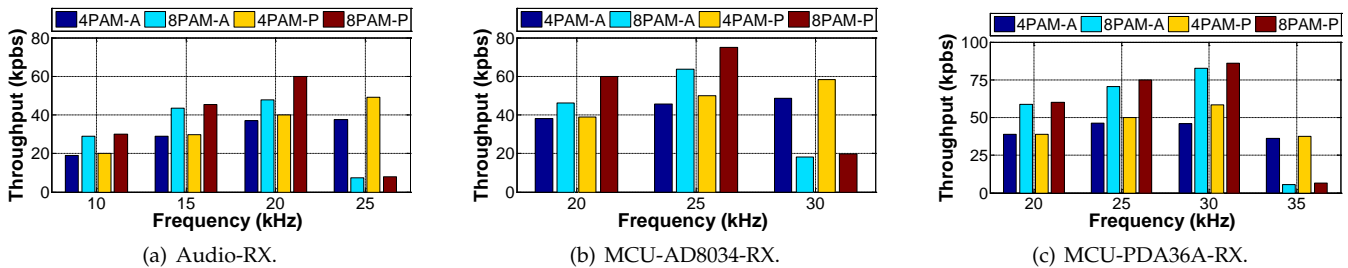(a) Audio-RX.   (b) MCU-AD8034-RX.   (c) MCU-PDA36A-RX.

Fig. 22. Throughput with a varying transmission frequency, where the postfix "-A" and "-P" refer to average and peak values, respectively.

receivers. Agreed with the results discussed in Section 3.2, changing the viewing angle within $60°$ slightly affects the channel quality as shown in Fig. 21. The two MCU-driven receivers have much better performance compared with Audio-RX, because Audio-RX has a reduced reception ability without an amplifier, we hence have to put it closer to the transmitter, which degrades the reception of the light from LED chips on the other side of the transmitter. Should we add a lens to focus the light emissions so as to improve the channel quality at around $0°$ (like most experimental settings), the channel quality would be drastically degraded at other angles. Although 4-PAM has slightly lower PERs than 8-PAM thanks to its larger symbol distance under all tests in Section 5.4, it may still be worth of using 8-PAM given its higher bit-symbol-ratio.

5.4.3 User Mobility

For a practical VLC system, users may freely wander under the VLC luminaires. We hence evaluate the demodulation performance of CoLight under mobile scenarios. We let a user hold CoLight's receivers towards the transmitter (keeping always LoS) for each experiment. We ask the user wander within the communication range of CoLight's transmitter to emulate potentially practical applications. To better evaluate the performance, we define three types of user moving patterns, namely, vertical moving (VM) (i.e., the user moves approaching or away the transmitter), parallel moving (PM) (i.e., the user moves parallelly with the transmitter) and hybrid moving (HM) (i.e., the user freely wanders). The speed of the user motion is around 0.8 m/s. We summarize the PER results in Table 1. Agreed with aforementioned evaluations, 4-PAM always outperforms 8-PAM in term of PER thanks to its larger symbol distance. Moreover, regular motion, e.g., VM or PM, clearly achieves a lower PER comparing to the freely wandering of HM, since free motion of the user may lead the VLC receiver even not capturing the transmitter successfully resulting in serious packet loss. Nevertheless, CoLight still maintains an acceptable PER which is sufficient for correctly decoding with our FEC of Raptor codes, and achievable data rates by CoLight can be found in Section 5.5.3.

5.5 Throughput

In this section, we report the achievable data rates by CoLight under various experiment settings.

5.5.1 Transmission Frequency

Within a reasonable frequency range studied in Section 5.4, the data rate of CoLight heavily depends on transmission frequency. As shown in Fig. 22, the throughput increases almost linearly with the transmission frequency, as every hertz carries a PAM symbol. In accordance with the observations made in Section 5.4.1 (where the same distance settings are taken), 4-PAM appears to be a more stable as the variances in throughput are small, whereas 8-PAM has a much higher peak rate in most cases, except when the frequency goes beyond the safe range (e.g., 35kHz for MCU-PDA36A-RX). In particular, Audio-RX achieves a maximum throughput up to 60 kbps (and an average of 40 kbps) with 8-PAM at a frequency of 20 kHz. As expected, the MCU-driven receivers achieve higher throughput comparing with Audio-RX, because they are not troubled by the coupling issue analyzed in Section 3.5 and 4. Consequently, the MCU-driven receivers yield a maximum throughput up to 80 kbps shown in Fig. 22(b) and 22(c), with an average throughput over 60 kbps.

5.5.2 Distance and View Angle

We now verify the data rate of CoLight from the application perspective, namely at varying distances and viewing angles. The throughput generally degrades with an increasing distance as shown in Fig. 23, but a simple PD without amplifier seems to have a threshold that throttles the performance of Audio-RX beyond 0.7 m. However, Audio-RX still reaches a peak throughput up to 60 kbps (with an average value beyond 40 kbps) at 0.7 m with 8-PAM as reported in Fig. 23(a); this is more than $50\times$ of that (0.7 kbps at 0.4 m) reported in [27]. With a more powerful front-end amplification, MCU-PDA36A-RX reaches a maximum throughput almost 80 kbps (with an average value at 60 kbps) at 1.6 m shown in Fig. 23(c), comparable to latest proposals [35], [36] that require an MHz sample rate at the receiver side. As one may expect, given the channel quality results in Section 5.4.2, changing receiver's viewing

TABLE 2
Throughput under mobile scenarios

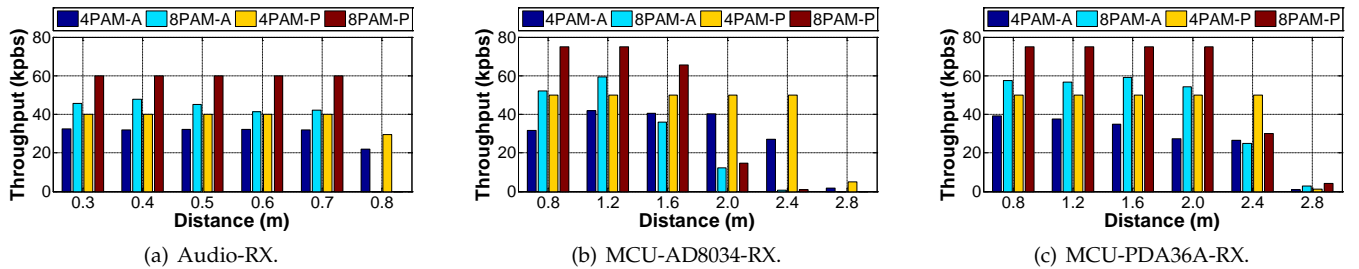|	Audio-RX			MCU-AD8034-RX			MCU-PDA36A-RX		
	VM	PM	HM	VM	PM	HM	VM	PM	HM
4-PAM (*kbps*)	20.2	19.6	17.7	23.0	22.0	18.6	22.0	23.6	23.0
8-PAM (*kbps*)	24.6	25.3	20.9	26.5	31.0	24.0	40.1	39.8	38.5

(a) Audio-RX.   (b) MCU-AD8034-RX.   (c) MCU-PDA36A-RX.

Fig. 23. Throughput with a varying distance, where the postfix "-A" and "-P" refer to average and peak values, respectively..

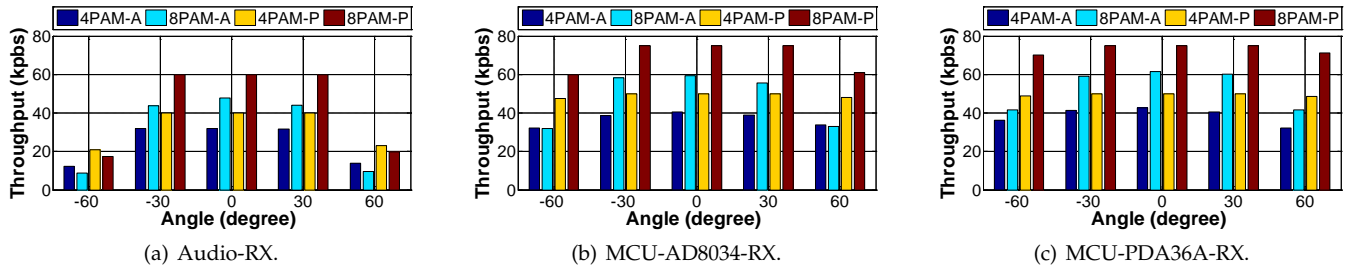(a) Audio-RX.   (b) MCU-AD8034-RX.   (c) MCU-PDA36A-RX.

Fig. 24. Throughput with a varying viewing angle, where the postfix "-A" and "-P" refer to average and peak values, respectively..

angle does not significantly affect on throughput for the two powerful MCU-driven receivers as shown in Fig. 24, and we can definitely improve the performance of Audio-RX by employing an amplifier. All these results strongly confirm the robustness of CoLight in real-life application scenarios.

5.5.3 User Mobility

We finally report the achievable data rate provided by CoLight for mobile users, while we present the channel property in term of PER in Section 5.4.3. We here report the average throughput for two adopted PAM modulations as presented in Table 2. Agreed with our above evaluations and analysis, 8-PAM has a higher throughput than 4-PAM thanks to its higher bit-symbol-ratio, whereas the 4-PAM has more stable communication comparing with 8-PAM for most cases given its larger symbol distance. Again, a good front-end design can definitely improve the data rate for mobile users based on our experiments by comparing with the throughput by MCU-AD8034-RX receiver. Nonetheless, our prototype of CoLight can deliver a throughput up to 40kbps for mobile users, which may be sufficient for realistic indoor VLC applications, e.g., broadcasting advertisements in a shopping mall.

5.6 Potentials and Limits: A Discussion

Receiver: Although CoLight suppresses the LED nonlinearity and can in principle reach up to 256-PAM, our current prototype utilizes only 4-PAM and 8-PAM. This mainly stems from the low sampling ability of the receivers, i.e., 44.1 kHz for audio interface and 200 kHz for MCU ADC. Therefore, one immediate solution to scale up the data rate is to increase the receivers' sampling ability, e.g., sample rate and resolution for supporting higher transmission

frequency and higher order modulation. For example, the audio interface of Samsung Galaxy S7 can support up to 192 kHz [37], and the ADC used by [36] reaches 3 MHz for supporting a transmission frequency of 100 kHz. Therefore, we believe that a more high-end receiver with stronger sampling ability has the potentials to acquire modulated signals with both high order modulation of up to 256-PAM and high transmission frequency, like what WiFi does.

Transmitter: In order to achieve a balanced complexity between transmitter and receiver, the transmitter needs to be upgraded accordingly. Increasing the transmission frequency beyond 100 kHz can be readily achieved by replacing transistors with MOSFETs, but such a straightforward improvement would demand a drastic increase in receiver sample rate, making the design even more unbalanced. To make a breakthrough, we need to leverage the direct digital-analog conversion ability of our transmitter, i.e., it converts the digital control signal to analog light intensity. Essentially, we may apply OFDM instead of PAM [38], and use the OFDM's IDFT output to directly drive the CoLight transmitter. As each OFDM subcarrier has a much narrower bandwidth, OFDM is much more robust against intersymbol interference due to the limited modulation bandwidth of COTS LEDs. This is probably the most efficient way to push VLC throughput to Mbps level in practice.

As a practical VLC transmitter, the unbalanced aging among LED chips should also be a concern besides chasing higher data rate. Although conventional DC balance coding mechanisms, e.g. 4B6B, can not deal with the heterogeneous aging of different LED chips on CoLight transmitter, the novel coding scheme proposed in [7] is exactly able to address it, because that coding scheme decomposes modulated

signals into Manchester codes at each LED group, which guarantees that all LED chips on the transmitter share an identical switch frequency.

Front-end: Our experiments clearly demonstrate that a good receiver front-end is crucial for improving the performance of CoLight (in terms of both data rate and communication distance), so we believe that a better design of the front-end should be another important factor. In particular, Audio-RX should gain a longer distance if it can have an amplifier, and we may indeed harvest energy from the audio jack (similar to [28]) to power the amplifier. Also, the MCU-driven receivers can use an automatic gain control amplifier to ensure a stable data rate at any distances within the transmitter's coverage. While using a more sensitive PD should certainly be considered (e.g., the avalanche photodetector adopted by [39]), it could be more effective if a blue filter and a lens are integrated with the PD to suppress the phosphorescent component (as used in [39], also refer to our discussions in Section 2.2).

Processing unit and algorithm: As the design of CoLight targets at combating LED nonlinearity to realize high-order modulations, it mostly relies on handy computing power and straightforward demodulation algorithms to handle the data processing. As a result, it has to trade bandwidth for robustness against PER. It should have a fairly large room to improve the data processing capabilities, such as a sequence detector rather than independently detecting each symbol. We could also make the system more complete by using high performance processing units (e.g., PRU on the Beaglebone platform used in [35], [36]) to handle computations.

6 RELATED WORK

Due to the space limit, we shall not give our focus on COTS VLC systems that rely either on screen-camera [40], [41], [42], [43], [44] or LED-camera [4], [18], [45], [15], [46], [19], [20], [6], as the former is quite irrelevant to what we study in this paper (as it is confined to application scenarios where a big screen is available), whereas the latter achieves at most a few kbps data rate confined by the low sampling rate of the smartphone cameras.

As we discussed earlier in Section 1, theoretical studies and experimental setups for VLC have been conducted for many years [10], [17], [22], [2], [11], [23], [21], [39], [12], [47], but they mostly rely on either modeling or highly specialized components, which distance themselves from practical applications. Nevertheless, inspirations could still be drawn from them to help us building COTS VLC systems, as some of these pioneering systems did achieve a Gbps level data rate. In particular, the idea of varying the number of LED chips to realize discrete luminance stepping was taken from [22], [23], [39], but CoLight stands out as a full-fledged system built purely from COTS components. Moreover, some proposals (e.g., [39]) also suggest certain specialized components that may be affordable to real-life applications and hence applicable to improve the performance of CoLight.

Applying PD to relax the receiver bottleneck for COTS VLC is still relatively new, and only a couple of attempts have been made. DarkLight [16] adopts a PD as the receiver

because it aims to perform VLC in darkness. The idea is to use very narrow pulses to carry data without really alighting an LED luminaire. However, this mechanism is nothing but the well known PPM modulation whose spectral efficiency is very low. SmartVLC [35] and Purple VLC [36] are the latest developments on this front. Though they achieve a throughput comparable to CoLight, they solely rely on frequency scaling to increase throughput, which, according to our discussion in Section 5.6, is rather inefficient. Nevertheless, the implementations reported by [35], [36] can be deemed as a complement to CoLight, as they explore the potential of elevating processing power from which we can directly draw lesson.

7 CONCLUSION

Aiming to bridge the performance gap between practical VLC systems and existing experimental setups, we have designed and presented CoLight in this paper. CoLight is a practical yet novel VLC system built purely upon COTS devices; it achieves a throughput up to 80 kbps. Essentially, CoLight relies on Combinational light emission to generate high-order modulations after eliminating the nonlinear effect of LEDs. Our compact circuit design for CoLight LED transmitter is able to generate high-order PAM symbols with only On-Off controls. Moreover, to handle LED diversity in massive circuit production, we have also invented an adaptive calibration scheme to automatically adjust light intensity for each PAM symbol. To get immediately usable VLC receivers for mobile devices, we have proceeded to directly interface a PD with a smartphone via its audio jack, and also to build two MCU-driven receivers emulating a potential integration into the phone. To suppress the AC coupling caused by the audio jack for achieving a high throughput, we have further proposed a delicate coding/decoding scheme. Using the CoLight prototypes with various receivers, we have demonstrated the practicality and promising performance of CoLight through extensive experiments.

Our strenuous design process along with the experiment evaluations has provided us with the firsthand knowledge about the potentials and limits of practical VLC systems, as discussed in Section 5.6. Based on some of these findings, we are on the way to improve our CoLight prototype: on one hand, adopting a more effective modulation scheme such as OFDM may further improve the data rate and/or communication reliability, and on the other hand, completing the prototype could be achieved by, for example, exploiting smartphone add-on modules like Moto-Mods [48].

REFERENCES

[1] Y. Yang, J. Luo, C. Chen, Z. Wen-De, and C. Liangyin, "SynLight: Synthetic Light Emission for Fast Transmission in COTS Device-enabled VLC," in *Proc. of the 38th IEEE INFOCOM*, 2019, pp. 1–9.

[2] X. Huang, Z. Wang, J. Shi, Y. Wang, and N. Chi, "1.6 Gbit/s Phosphorescent White LED based VLC Transmission Using A Cascaded Pre-Equalization Circuit and A Differential Outputs PIN Receiver," *OSA Opt. Express*, vol. 23, no. 17, pp. 22 034–22 042, 2015.

[3] B. Weir, "Driving The 21st Century's Lights," *IEEE Spectrum*, vol. 49, no. 3, 2012.

[4] C.-L. Chan, H.-M. Tsai, and K. C.-J. Lin, "POLI: Long-Range Visible Light Communications Using Polarized Light Intensity Modulation," in *Proc. of the 15th ACM MobiSys*, 2017, pp. 109–120.

[5] C.-W. Chow, C.-Y. Chen, and S.-H. Chen, "Visible Light Communication Using Mobile-Phone Camera with Data Rate Higher Than Frame Rate," *OSA Opt. Express*, vol. 23, no. 20, pp. 26 080–26 085, 2015.

[6] Y. Yang, J. Nie, and J. Luo, "ReflexCode: Coding with Superposed Reflection Light for LED-Camera Communication," in *Proc. of the 23rd ACM MobiCom*, 2017, pp. 193–205.

[7] Y. Yang and J. Luo, "Boosting the Throughput of LED-Camera VLC via Composite Light Emission," in *Proc. of the 37th IEEE INFOCOM*, 2018, pp. 315–323.

[8] C.-W. Chow, R.-J. Shiu, Y.-C. Liu, X.-L. Liao, K.-H. Lin, Y.-C. Wang, and Y.-Y. Chen, "Using advertisement light-panel and CMOS image sensor with frequency-shift-keying for visible light communication," *Opt. Express*, vol. 26, no. 10, pp. 12 530–12 535, May 2018.

[9] C. Chow, R. Shiu, Y. Liu, C. Yeh, X. Liao, K. Lin, Y. Wang, and Y. Chen, "Secure mobile-phone based visible light communications with different noise-ratio light-panel," *IEEE Photonics Journal*, vol. 10, no. 2, pp. 1–6, 2018.

[10] H. Elgala, R. Mesleh, and H. Haas, "An LED Model for Intensity-Modulated Optical Communication Systems," *IEEE Photon. Technol. Lett.*, vol. 22, no. 11, pp. 835–837, 2010.

[11] B. Inan, S. J. Lee, S. Randel, I. Neokosmidis, A. M. Koonen, and J. W. Walewski, "Impact of LED Nonlinearity on Discrete Multitone Modulation," *IEEE/OSA J. Opt. Commun. Netw.*, vol. 1, no. 5, pp. 439–451, 2009.

[12] K. Ying, Z. Yu, R. J. Baxley, H. Qian, G.-K. Chang, and G. T. Zhou, "Nonlinear Distortion Mitigation in Visible Light Communications," *IEEE Wireless Commun.*, vol. 22, no. 2, pp. 36–45, 2015.

[13] H. Elgala, R. Mesleh, and H. Haas, "Non-Linearity Effects and Predistortion in Optical OFDM Wireless Transmission Using LEDs," *Inderscience International Journal of Ultra Wideband Communications and Systems*, vol. 1, no. 2, pp. 143–150, 2009.

[14] H. Qian, S. Yao, S. Cai, and T. Zhou, "Adaptive Postdistortion for Nonlinear LEDs in Visible Light Communications," *IEEE Photon. J.*, vol. 6, no. 4, pp. 1–8, 2014.

[15] J. Hao, Y. Yang, and J. Luo, "CeilingCast: Energy Efficient and Location-bound Broadcast through LED-Camera Communication," in *Proc. of the 35th IEEE INFOCOM*, 2016, pp. 1–9.

[16] Z. Tian, K. Wright, and X. Zhou, "The DarkLight Rises: Visible Light Communication in the Dark," in *Proc. of the 22nd ACM MobiCom*, 2016, pp. 2–15.

[17] B. Fahs, M. Romanowicz, and M. M. Hella, "A Gbps Building-to-Building VLC Link Using Standard CMOS Avalanche Photodiodes," *IEEE Photon. J.*, vol. 9, no. 6, pp. 1–9, 2017.

[18] C. Danakis, M. Afgani, G. Povey, I. Underwood, and H. Haas, "Using a CMOS Camera Sensor for Visible Light Communication," in *2012 IEEE Globecom Workshops*, 2012, pp. 1244–1248.

[19] Y.-S. Kuo, P. Pannuto, K.-J. Hsiao, and P. Dutta, "Luxapose: Indoor Positioning with Mobile Phones and Visible Light," in *Proc. of the 20th ACM MobiCom*, 2014, pp. 447–458.

[20] H. Lee, H. Lin, Y. L. Wei, H. I. Wu, H. M. Tsai, and K. Lin, "Rolling-Light: Enabling Line-of-Sight Light-to-Camera Communications," in *Proc. of 13th ACM MobiSys*, 2015, pp. 167–180.

[21] D. Tsonev, H. Chun, S. Rajbhandari, J. J. McKendry, S. Videv, E. Gu, M. Haji, S. Watson, A. E. Kelly, G. Faulkner *et al.*, "A 3-Gb/s single-LED OFDM-based Wireless VLC Link Using a Gallium Nitride μLED," *IEEE Photon. Technol. Lett.*, vol. 26, no. 7, pp. 637–640, 2014.

[22] T. Fath, C. Heller, and H. Haas, "Optical Wireless Transmitter Employing Discrete Power Level Stepping," *J. Lightw. Technol.*, vol. 31, no. 11, pp. 1734–1743, 2013.

[23] J. Li, Z. Huang, R. Zhang, F. Zeng, M. Jiang, and Y. Ji, "Superposed Pulse Amplitude Modulation for Visible Light Communication," *OSA Opt. Express*, vol. 21, no. 25, pp. 31 006–31 011, 2013.

[24] "Thorlabs PDA10A Si Fixed Gain Detector," https://www.thorlabs.com/thorProduct.cfm?partNumber=PDA10A.

[25] C.-H. Yeh, Y.-L. Liu, and C.-W. Chow, "Real-Time White-Light Phosphor-LED Visible Light Communication (VLC) with Compact Size," *OSA Opt. Express*, vol. 21, no. 22, pp. 26 192–26 197, 2013.

[26] "Toshiba TLP293-4(GB-TP,E," https://www.mouser.com/ds/2/408/TLP293-4_datasheet_en_20151021-737014.pdf.

[27] S. Schmid, D. Schwyn, K. Aksit, G. Corbellini, T. R. Gross, and S. Mangold, "From Sound to Sight: Using Audio Processing to Enable Visible Light Communication," in *2014 IEEE Globecom Workshops*, 2014, pp. 518–523.

[28] S. Verma, A. Robinson, and P. Dutta, "AudioDAQ: Turning the Mobile Phone's Ubiquitous Headset Port into a Universal Data Acquisition Interface," in *Proc. of the 10th ACM SenSys*, 2012, pp. 197–210.

[29] L. Li, P. Hu, C. Peng, G. Shen, and F. Zhao, "Epsilon: A Visible Light Based Positioning System," in *Proc. of 11th USENIX/ACM NSDI*, 2014, pp. 331–343.

[30] T. Komine and M. Nakagawa, "Fundamental Analysis for Visible-Light Communication System Using LED Lights," *IEEE Trans. Consum. Electron.*, vol. 50, no. 1, pp. 100–107, 2004.

[31] "PDA36A-EC - Si Switchable Gain Detector," https://www.thorlabs.com/thorproduct.cfm?partnumber=PDA36A-EC.

[32] S. Rajagopal, R. Roberts, and S. Lim, "IEEE 802.15.7 Visible Light Communication: Modulation Schemes and Dimming Support," *IEEE Commun. Mag.*, vol. 50, no. 3, pp. 72–82, 2012.

[33] "Low Cost, 80 MHz FastFET Op Amps," http://www.analog.com/media/en/technical-documentation/data-sheets/AD8033_8034.pdf.

[34] A. Shokrollahi, "Raptor Codes," *IEEE Trans. Inf. Theory*, vol. 52, no. 6, pp. 2551–2567, 2006.

[35] H. Wu, Q. Wang, J. Xiong, and M. Zuniga, "SmartVLC: When Smart Lighting Meets VLC," in *Proc. of the 13th ACM CoNEXT*, 2017, pp. 212–223.

[36] S. Yin, N. Smaoui, M. Heydariaan, and O. Gnawali, "Purple VLC: Accelerating Visible Light Communication in Room Area through PRU Offloading," in *Proc. of the 15th EWSN*, 2018, pp. 67–78.

[37] "Samsung Galaxy S7 edge," https://www.gsmarena.com/samsung_galaxy_s7_edge-7945.php.

[38] Y. Yang, C. Chen, P. Du, X. Deng, J. Luo, W.-D. Zhong, and L. Chen, "Low complexity ofdm vlc system enabled by spatial summing modulation," *Opt. Express*, vol. 27, no. 21, pp. 30 788–30 795, 2019.

[39] C. Xi, A. Mirvakili, and V. J. Koomson, "A Visible Light Communication System Demonstration Based on 16-level Pulse Amplitude Modulation of an LED Array," in *Proc. of the IEEE SOPO 2012*, 2012, pp. 1–4.

[40] W. Hu, H. Gu, and Q. Pu, "Lightsync: Unsynchronized Visual Communication over Screen-Camera Links," in *Proc. of the 19th ACM MobiCom*, 2013, pp. 15–26.

[41] W. Hu, J. Mao, Z. Huang, Y. Xue, J. She, K. Bian, and G. Shen, "Strata: Layered Coding for Scalable Visual Communication," in *Proc. of the 20th ACM MobiCom*, 2014, pp. 79–90.

[42] T. Li, C. An, X. Xiao, A. T. Campbell, and X. Zhou, "Real-time Screen-Camera Communication Behind Any Scene," in *Proc. of the 13th ACM MobiSys*, 2015, pp. 197–211.

[43] S. Perli, N. Ahmed, and D. Katabi, "PixNet: Interference-Free Wireless Links using LCD-Camera Pairs," in *Proc. of the 16th ACM MobiCom*, 2010, pp. 137–148.

[44] A. Wang, Z. Li, C. Peng, G. Shen, G. Fang, and B. Zeng, "Inframe++: Achieve Simultaneous Screen-Human Viewing and Hidden Screen-Camera Communication," in *Proc. of the 13th ACM MobiSys*, 2015, pp. 181–195.

[45] H. Du, J. Han, X. Jian, T. Jung, C. Bo, Y. Wang, and X.-Y. Li, "Martian: Message Broadcast via LED Lights to Heterogeneous Smartphones," *IEEE J. Sel. Areas Commun.*, vol. 35, no. 5, pp. 1154–1162, 2017.

[46] P. Hu, P. H. Pathak, X. Feng, H. Fu, and P. Mohapatra, "Colorbars: Increasing Data Rate of LED-to-Camera Communication Using Color Shift Keying," in *Proc. of the 11th ACM CoNEXT*, 2015, p. 12.

[47] R. Zhang, H. Claussen, H. Haas, and L. Hanzo, "Energy Efficient Visible Light Communications Relying on Amorphous Cells," *IEEE J. Sel. Areas Commun.*, vol. 34, no. 4, pp. 894–906, 2016.

[48] "Motorola Moto Mods," https://www.motorola.com/us/moto-mods.

Yanbing Yang received his B.E. and M.E. degrees from University of Electronic Science and Technology of China, China, and his Ph.D degree in Computer Science and Engineering from Nanyang Technological University, Singapore. He is currently an Associate Research Professor in College of Computer Science, Sichuan University, China. His research interests include IoT, visible light communication, visible light sensing, as well as their applications.

Wen-De Zhong was a Post-Doctoral Fellow with NTT Network Service and System Laboratories, Japan, from 1993 to 1995. He was a Senior Research Fellow with the Department of Electrical and Electronic Engineering, University of Melbourne, Australia, from 1995 to 2000. He joined Nanyang Technological University, Singapore, in 2000, as an Associate Professor and became a Full Professor in 2009, and is currently with the School of Electrical and Electronic Engineering. He has co-authored over 250 refereed journal and conference papers. His current research interests include visible light communication/positioning, optical fiber communication systems and networks, optical access networks, and signal processing. He has served on organizing and/or technical program committee for numerous international conferences, including ECOC, ICC, GLOBECOM, OECC, ICICS, and ICOCN. He is currently an Associate Editor of the IEEE ACCESS and also an Editor of Unmanned Systems.

Jun Luo received his BS and MS degrees in Electrical Engineering from Tsinghua University, China, and the Ph.D. degree in Computer Science from EPFL (Swiss Federal Institute of Technology in Lausanne), Lausanne, Switzerland. From 2006 to 2008, he has worked as a postdoctoral research fellow in the Department of Electrical and Computer Engineering, University of Waterloo, Waterloo, Canada. In 2008, he joined the faculty of the School Of Computer Science and Engineering, Nanyang Technological University in Singapore, where he is currently an Associate Professor. His research interests include mobile and pervasive computing, wireless networking, applied operations research, as well as network security. More information can be found at http://www.ntu.edu.sg/home/junluo.

Liangyin Chen received the Ph.D degree in Computer Science from Sichuan University, China, where he is currently a Professor. He was a visiting researcher at the University of Minnesota from August 2009 to September 2010 under the guidance of Professor Tian He. His research interests include wireless sensor network, embedded systems, computer network, distributed systems, big data analysis, and natural language processing.

Chen Chen received both the B.S. and M.Eng. degrees from University of Electronic Science and Technology of China, Chengdu, China, in 2010 and 2013, respectively, and the Ph.D. degree from Nanyang Technological University, Singapore, in 2017. He worked as a postdoctoral researcher in the School of Electrical and Electronic Engineering, Nanyang Technological University from 2017 to 2019. He is currently a tenure-track assistant professor in the School of Microelectronics and Communication Engineering, Chongqing University, China. His research interests include visible light communications, LiFi, visible light positioning, optical access networks, and digital signal processing.

Zequn Chen Zequn Chen is now an undergraduate student in the College of Computer Science of Sichuan University. His research interests include visible light communication and positioning.